TASR Trends in Applied Sciences Research

OPEN ACCESS

# Coconut Shell Biochar: Physicochemical Textural Properties, Morphology, and Carbon Sequestration Potential

*Chima Maximus Ejimadu, James Majebi Okuo, and Felix Ebhodaghe Okieimen*
*University of Benin, Department of Chemistry, Centre for Biomaterials Research, Benin, Nigeria*

*Corresponding Author*: Chima Maximus Ejimadu (ejimaduchima@gmail.com)

**ABSTRACT**

**Background and Objective:** Coconut shell biochar (CSB) is a promising soil amendment and carbon sequestration material, yet its physicochemical and textural properties, stability, and carbon sequestration potential under different pyrolysis temperatures remain underexplored. This study aimed to investigate the effects of slow pyrolysis temperature on the physicochemical, textural, and morphological characteristics of coconut shell biochars, and to assess their carbon sequestration potential. **Materials and Methods:** Coconut shells were pyrolyzed at 350, 450, and 700°C to produce biochars, which were characterized for yield (%), pH, bulk density, cation exchange capacity, electrical conductivity, surface functional groups, and BET textural properties (specific surface area, pore volume, and pore size). Surface morphology and elemental composition were analyzed using SEM/EDX. Carbon sequestration potential was estimated from ultimate analysis and validated via accelerated chemical oxidation using $KMnO_4$. **Results:** Biochar properties were strongly temperature-dependent. Increasing pyrolysis temperature enhanced pH, electrical conductivity, and cation exchange capacity, while decreasing yield and bulk density. Total surface functional groups declined from 4.04 mmol/g (CSB350) to 2.17 mmol/g (CSB700). Specific surface area increased from 282.0 $m^2/g$ (CSB350) to 712.0 $m^2/g$ (CSB450) before decreasing to 320.7 m/g (CSB700). Pore diameter increased from 2.80 nm to 4.85 nm, and pore volume peaked at 0.36 $cm^3/g$ for CSB450. H:C and O:C ratios decreased with pyrolysis, from 0.71 and 0.58 in raw shell to 0.40 and 0.30 in CSB700, indicating high long-term stability (>100 years) on the IBI scale. Accelerated chemical oxidation results corroborated these findings, confirming the relationship between pyrolysis temperature and biochar stability. **Conclusion:** Coconut shell biochar exhibits temperature-dependent physicochemical and textural properties, with higher pyrolysis temperatures favoring stability and carbon sequestration. These findings support the use of CSB as a long-lasting soil amendment and highlight its potential to mitigate atmospheric carbon. Future studies should explore field-scale impacts on soil properties and crop productivity.

**KEYWORDS**

Coconut shell biochar, textural properties, carbon sequestration, chemical oxidation stability, ultimate analysis



ISSN: 2151-7908 (Online)
ISSN: 1819-3579 (Print)
https://doi.org/10.3923/tasr.2026.01.13

Received: 31 Dec. 2025
Accepted: 15 Apr. 2026
Published: 20 May, 2026

## INTRODUCTION

There is widespread and growing interest in biomass as an alternative resource for energy, chemicals and materials to substitute and/or supplement the current finite, high-cost, eco-intrusive and eco-damaging petroleum based resources. Biomass, in addition to being environmentally benign, is available at low-cost in all regions of the world; making it supply free of local or regional social-political perturbations. Pyrolysis, as an aspect of thermochemical technology is a proven, simple and flexible procedure that has been used to convert biomass into chemicals and fuels[1]. Pyrolysis can, on the basis of heat treatment temperature, duration of heat treatment and heating rate, be considered as slow, fast as flash pyrolysis. While slow pyrolysis yields mainly solid biochar product (up to 60 wt%), the products from fast and flash pyrolysis are mainly bio-oil (60-70%) and biogas (25-30%)[2]. Pyrolysis temperature (highest heat treatment temperature) is widely considered the most important process variable affecting the properties and applications of biochar[3-5]. During pyrolysis of biomass a series of reactions (changes) occur as pyrolysis temperature increases: Degradation, decarboxylation and decarbonylation, leading to distinct char phases and physical states, including changes in the structure of biochar[6]. These changes are inherently linked with changes in the physicochemical and textural properties of the biochar as well as its morphology and chemical composition[7]. On account of the potential multifunctional application of biochar[8,9], several biomass materials, including crop residues, wood etc. have been utilized in biochar production[9,10,11]. Previous works on the pyrolysis of coconut shell biomass were summarized in a recent report[12]. It is estimated that about 124 million tons of coconut husk are generated by the coconut industry annually[13]. These waste materials are often disposed indiscriminately into the environment or/and burnt in-open-air, both with considerable environmental and public health concerns[14]. Although coconut shell-derived activated carbon has found use in adsorptive application for the removal of organic an inorganic contaminant from wastewater[3], the change in properties associated with pyrolysis temperature have made biochar a material of interest in diverse applications. However, the effect of pyrolysis temperature on the properties of coconut shell biochar relevant to its multifunctional applications has not been widely reported.

Pyrolytic conversion of coconut shell biomass to biochar will in addition to providing a more environmentally friendly treatment method for this waste stream, it would lead to the production of higher value end-product. Hence, this study aims to investigate coconut shell biochar with emphasis on its physicochemical and textural properties, morphology, and carbon sequestration potential, in order to evaluate its suitability for environmental applications and long-term carbon storage.

## MATERIALS AND METHODS

**Study area:** The coconut shells were collected between December 2022 and February 2023 from the local market in Benin City. The market is in Uselu area of Egor Local Government Area, Edo State, Nigeria (approximately 6.34°N, 5.63°E) and is located in the South Region of Nigeria.

**Materials:** The coconut shells were washed repeatedly with tap water and rinsed with distilled water to remove physical impurities, then air-dried at room temperature for seven days. The dried coconut shells were crushed to a particle size of 2 mm and thereafter pyrolysed at heat treatment temperatures of 350, 400, 450, 500, 600, and 700°C, at heating rate of 10°C/min and held for 30 min at the highest heating treatment temperature. The resulting biochars were crushed and sieved through a 250 µm mesh and transferred into airtight containers. They were labeled as CSB (coconut shell biochar), BC350, BC400, BC450, BC500, BC600, and BC700, respectively. Figure 1 illustrates the preparation process of the coconut shell biochar. The chemicals used were of analytical grade.

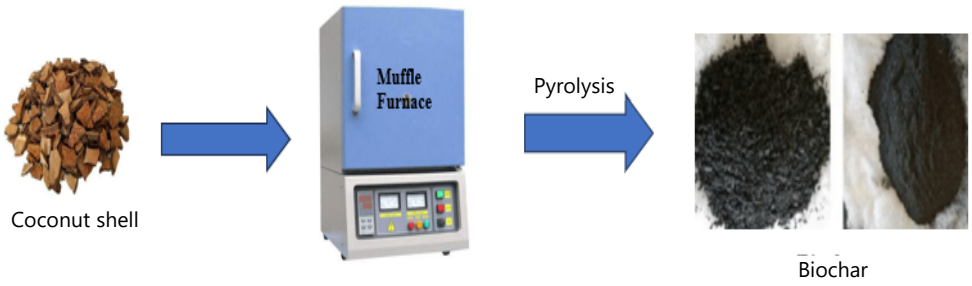


Fig. 1: Preparation process of coconut shell biochar

**Physicochemical characterization**

**Determination of yield (wt%):** The biochar yield was determined using the formula as described by Naeem *et al.*[15]:

$$\text{Biochar yield (w\%)} = \frac{\text{Weight of biochar}}{\text{Weight of feedstock used}} \times 100 \quad (1)$$

**Determination of pH and electrical conductivity:** The pH was measured in deionized water using 1:5 ratio. Samples were thoroughly mixed and allowed to stand for 1hr. The pH was measured with a precalibrated digital pH meter (Jenway 3020, DUNMOW ESSEX, JENWAY LTD., England).

The electrical conductivity (EC) of the biochar slurry was determined. A mixture of biochar and deionized water in a 1:10 ratio was agitated for 1 hr; allowed to stand for 30 minutes, and the EC of the suspension was measured using a precalibrated conductivity meter (DDS-307, Search Tech. Instrument, No. X619070942).

**Bulk density:** Bulk density was determined using the tapping method as described by Ahmedna *et al.*[17] in duplicates and the average value was used to calculate bulk density (Eq. 2):

$$\text{Bulk density (g.cm}^{-3}) = \frac{\text{Weight of dry sample}}{\text{Volume of packed dry material (cm}^3)} \quad (2)$$

**Cation exchange capacity (CEC):** The CEC was determined using the modified ammonium acetate displacement method as described by Othugile *et al.*[18]. Samples (0.2 g each) were leached five times with 20 mL deionized water to reduce interference from soluble salts. The samples were then leached five times with 20 mL of 1M sodium acetate (pH 7), to remove or extract exchangeable cations. The samples were later washed with 20 mL of ethanol five times to remove the excess sodium ion. The $Na^+$ on the exchangeable sites of the material was then displaced five times using 100 mL of 1M Ammonium acetate (pH 7). The CEC was calculated from the $Na^+$ displaced by $NH_4^+$, measured using a flame photometer.

**Surface morphology and elemental composition:** The Scanning Electron Microscope (SEM, Hitachi SU 3500 scanning microscope, Tokyo) and an Energy Dispersive X-ray Spectrometer (EDX) were used in combination to analyze the surface morphology of the produced samples and determine their elemental composition, and performed in 2023-2024.

**Determination of surface area:** The surface area of the samples was determined using the nitrogen adsorption-desorption method based on the Brunauer–Emmett–Teller (BET) theory. 0.3 g of each of the samples was placed in a BET glass tube and weighed before and after loading. The samples were degassed at 473 K for 3 hrs using a Micromeritics FlowPrep 060 system under a flow of nitrogen gas to remove physically adsorbed moisture and gases. After degassing, the samples were reweighed and the analysis

was carried out in micromeritics Tristar 3000 V4.02 under liquid nitrogen temperature where BET surface area and pore volume/size of the samples were automatically calculated by the instrument using Nitrogen adsorption-desorption isotherms and the results were recorded on the computer attached to the instrument[19,20].

**Ultimate analysis:** The percentages of C, H, S, and N in biochars were determined with an elemental analyzer (Elemental Vario EL III, Germany), and the O content was calculated by subtracting C, H, N, S, and ash contents from the total[21].

**Chemical oxidation stability:** The $KMnO_4$ method described by Tirol-Padre and Ladha[22], was used to assess the easily oxidizable fraction of the studied biochars. Biochar samples were acid pretreated to remove inorganic carbonates following the method described by Fidel *et al.*[23]. Typically, the biochar was added to a solution of $KMnO_4$ (33mM, pH 7.2) in a 1:50 w/v biochar: $KMnO_4$ ratio. It was agitated for 60 min, heated at about 60°C for 60 min and thereafter left overnight at 25°C. The solid residue was separated, rinsed with distilled water, and dried at 80°C for 4 days. The mass loss from the oxidation treatment was measured gravimetrically, and the dried sample was subsequently analyzed for its elemental composition (C, H, N, O, and S).

An indication of the stability of biochar to oxidative degradation AE may be obtained from Eq. 3:

$$AE = \frac{Br \times Brc}{Bt \times Btc} \times 100 \quad (3)$$

where, BrC and BtC represent the carbon content in the residual and total biochar, respectively, and Br and Bt are the mass after and before treatment[24].

## RESULTS AND DISCUSSION

**Biochar physicochemical properties:** Figure 2 shows the dependence of biochar yield and the measured physicochemical properties on heat treatment temperatures (HTT).

Figure 2a show that the yield of biochar decreased markedly from 67.70±0.50% at heat treatment temperature of 350°C to 35.76 ± 0.42% at 700°C. This decrease in biochar yield agrees with results of previous workers and has been attributed to decomposition of biomass and secondary decomposition of biochar residue; charring and devolatilization reaction that occur at heat treatment temperature[25]. It can seen from Fig. 2a that cation exchange capacity (CEC) (cmol/kg) showed an initial increase with increase in heat treatment temperature from 11.49±2.43 at 350°C to 28.03±2.00 at 450°C; a more than two-fold increase, and then decreased at higher heat treatment temperature to 14.11±2.50 at 700°C an overall increase in CEC value of about 23% within the range of heat treatment temperature. The higher values of CEC of biochar obtained at moderate temperatures (>350°C<500°C) suggest that coconut shell biochars obtained within this range of temperature may be more suited for soil application for agronomic benefits. Figure 2a also showed that electrical conductivity (ms./cm) of the biochar samples increased with increasing heat treatment temperature from 5.12 at 350°C to 25.60 at 700°C; i.e for the two-fold increase in heat treatment temperature, the electrical conductivity value of the biochar increased 5-fold. This increase in EC with increasing heat treatment temperature may be due to loss of volatiles and the concentration of elements in the biochar residue[26]. Figure 2b shows that increase in heat treatment temperature was associated with increase in pH and a decrease in bulk density of biochar samples. The increase of pH with heat treatment temperature has been explained in terms of the decrease in organic functional groups e.g. -OH and -COOH, which influence the pH of biochar accumulation of inorganic salts of sodium, potassium, magnesium and calcium as carbonates generated at higher heat treatment temperature[27]. It has been reported that application of biochar with high pH in acidic soil can improve

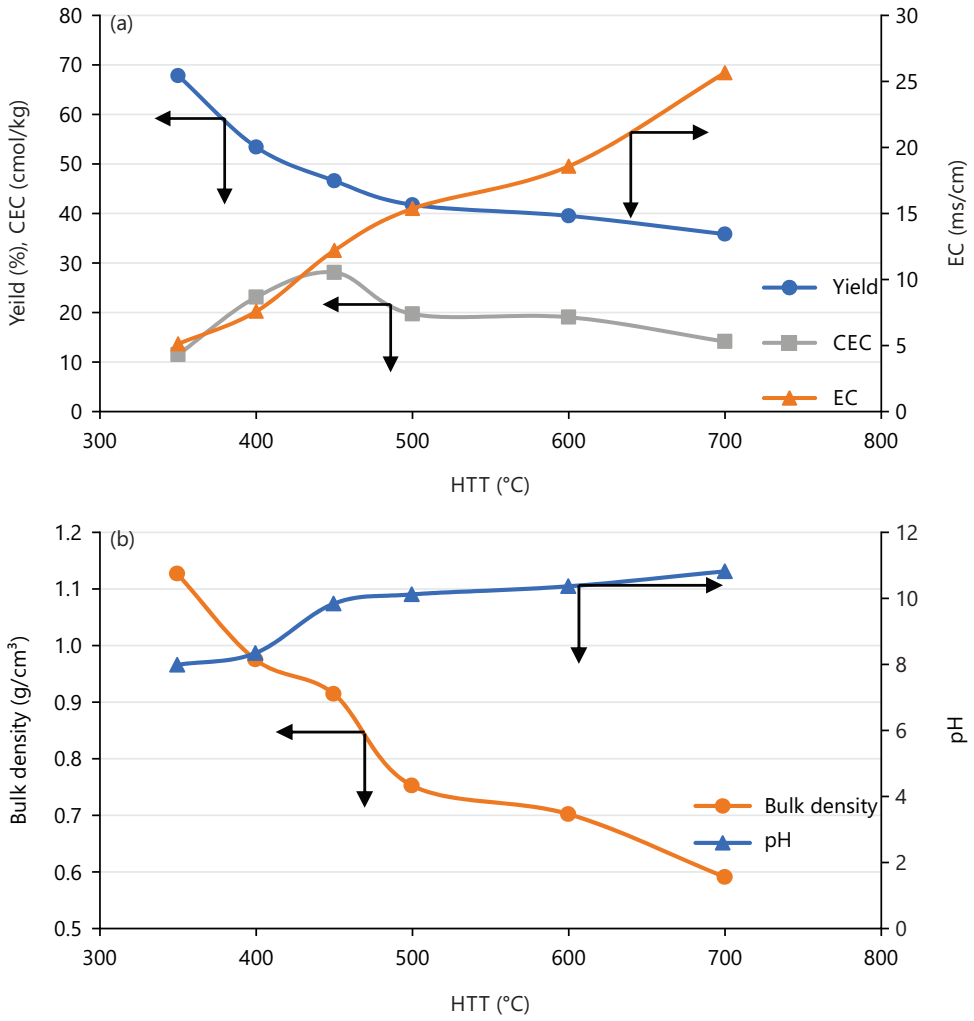


Fig. 2: Effect of heat treatment temperature (HTT) on a) yield, electrical conductivity (EC) and cation exchange capacity (CEC); b) bulk density and pH

cation exchange capacity, attain greater neutralization and reduce green house gas emissions[28]. Therefore coconut shell biochar prepared at high temperature range maybe suitable for amendments of acidic soil with agronomic benefits; reduce soil nutrient leaching, and improve soil nutrient availability. The bulk density ($g.cm^{-3}$) of biochar samples was low and decreased from 1.12±0.22 for 350°C to 0.59±0.15 at 700°C. Similar decrease in bulk density of biochar with increase in heat treatment temperature was reported by Weber and Quicker[29], and explanations in terms of changes in the structure biochar with increase in heat treatment temperatures were proffered.

**Surface acid functional groups:** Total surface oxygen functional groups (mmol/g): Carboxylic, lactonic and phenolic groups of biochar samples is shown in Fig. 3 as a function of heat treatment temperature (HTT).

The result in Fig. 3 show that the total surface oxygen functional groups decrease from 4.94 for biochar prepared at 350°C to 2.17 for biochar prepared at 700°C. This trend is similar to that reported by Ogede *et al.*[30], and explanations in terms of increased volatilization of surface groups at higher temperatures. Surface acid functional groups are also implicated in retention capacity of nutrient elements. These results indicate a negative correlation between surface oxygen functional groups and heat treatment temperature and the capacity of biochars to retain mineral nutrients.

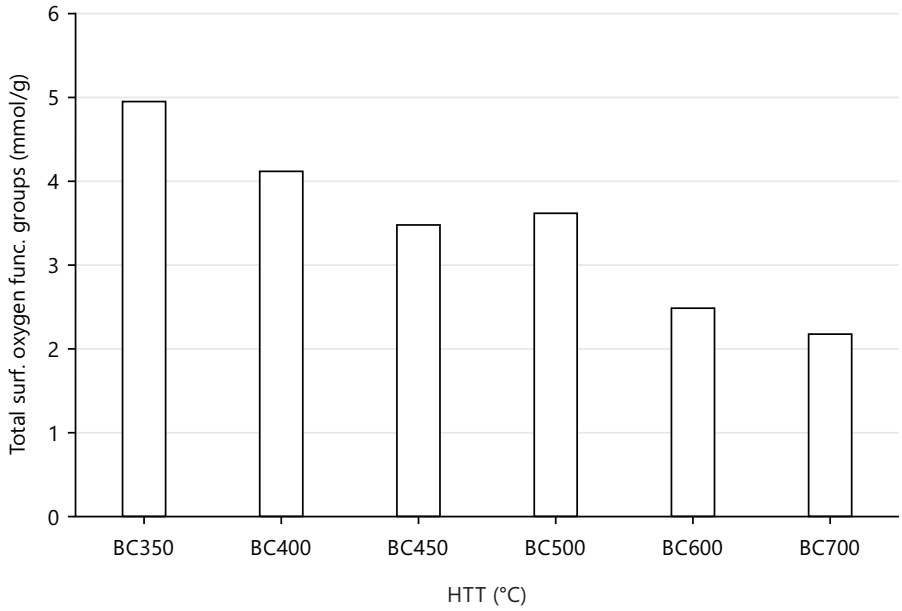


Fig. 3: Effect of heat treatment temperature (HTT) on the total surface oxygen functional groups on coconut shell biochar

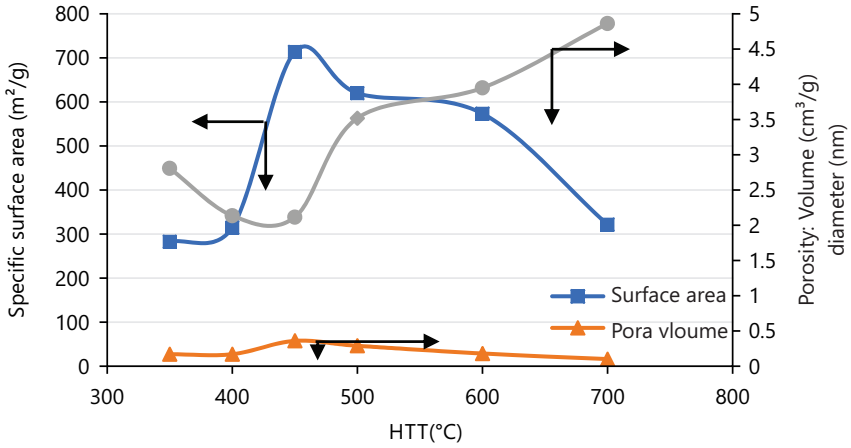


Fig. 4: Textural Properties of coconut shell biochar obtained at different heat treatment temperature (HTT)

**Textural properties:** The textural properties, specific surface area ($m^2/g$), pore diameter (nm), and pore volume ($cm^3/g$) of coconut shell biochar obtained at different heat treatment temperatures are shown in Fig. 4.

Specific surface area, porosity and pore volume are important parameters for characterizing materials. It can be seen that the specific surface area increased from 282.00 at heat treatment temperature 350°C to 712.00 at 450°C a two-fold increase, followed a gradual decrease in specific surface area at higher temperatures and then to 320.70 at 700°C. The range of values obtained for the pore diameter of the biochars; 2.80 nm for 350°C and 4.50 nm for 700°C indicate the samples are mesoporous. The pore volume of the biochar samples varied from 0.17 $cm^3/g$ for 350°C to 0.10 $cm^3/g$ for 700°C. Heat treatment temperature of coconut shell at 500°C gave biochar with highest specific surface area 712.00 $m^2/g$ and pore volume 0.29 $cm^3/g$, while pore size was highest for the biochar sample obtained at the heat treatment temperature of 700°C. Textural properties are interconnected and they have significant impact on the performance of porous materials such as biochars in various applications.

(a)

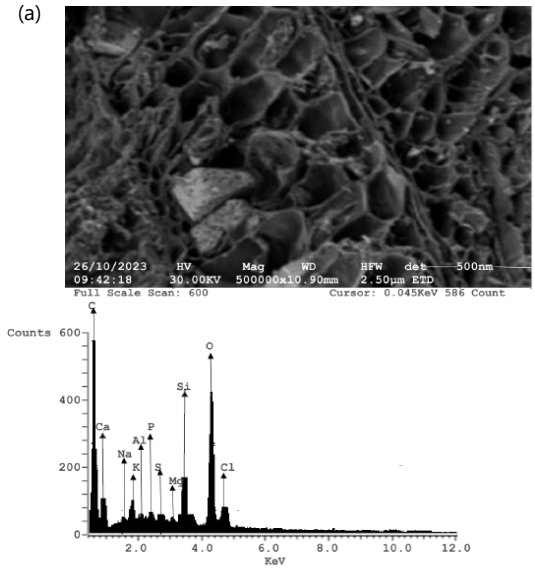


| Elements | Composition (%) |
|---|---|
| C | 60.50 |
| O | 29.72 |
| Ca | 1.15 |
| Si | 3.01 |
| Al | 0.20 |
| K | 1.76 |
| Na | 0.78 |
| Mg | 0.56 |
| P | 1.04 |
| Cl | 1.16 |
| S | 0.11 |

(b)

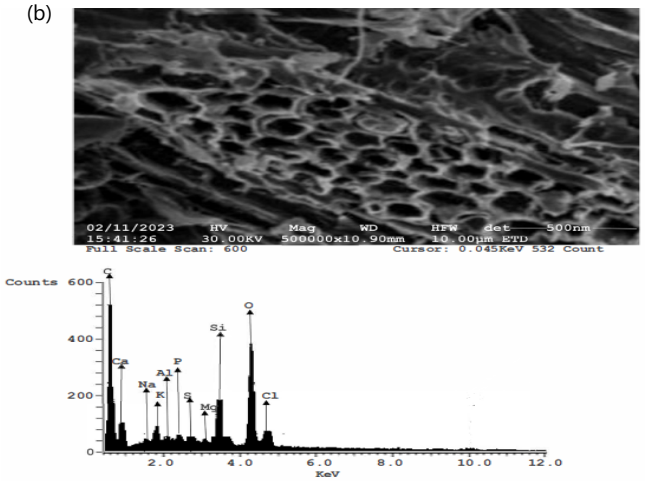


| Elements | Composition (%) |
|---|---|
| C | 63.1 |
| O | 24.07 |
| Ca | 1.87 |
| Si | 3.51 |
| Al | 0.49 |
| K | 2.06 |
| Na | 1.12 |
| Mg | 0.87 |
| P | 1.24 |
| Cl | 1.49 |
| S | 0.15 |

(c)

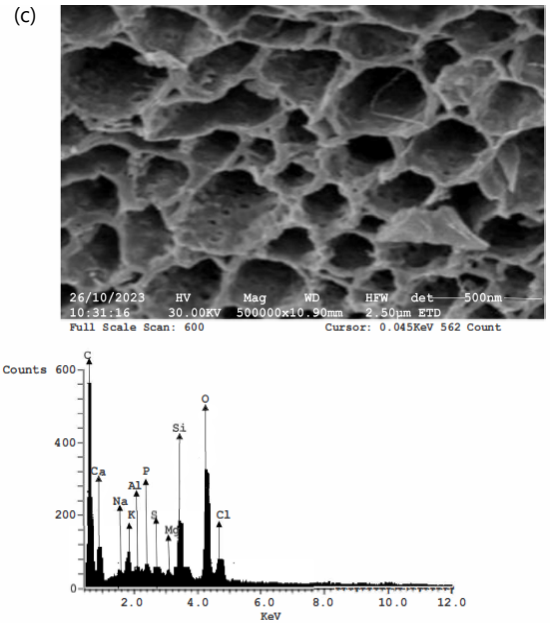


| Elements | Composition (%) |
|---|---|
| C | 66.03 |
| O | 18.40 |
| Ca | 2.02 |
| Si | 3.92 |
| Al | 0.91 |
| K | 2.11 |
| Na | 1.55 |
| Mg | 1.50 |
| P | 1.34 |
| Cl | 2.09 |
| S | 0.12 |

Fig 5(a-f): Continue

(d)

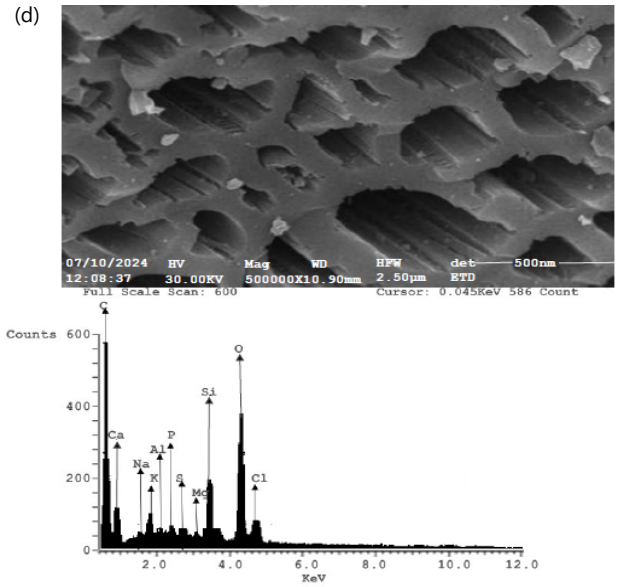


| Elements | Composition (%) |
|---|---|
| C | 65.15 |
| O | 17.13 |
| Ca | 1.47 |
| Si | 6.17 |
| Al | 1.11 |
| K | 2.31 |
| Na | 1.73 |
| Mg | 1.11 |
| P | 1.59 |
| Cl | 2.11 |
| S | 0.10 |

(e)

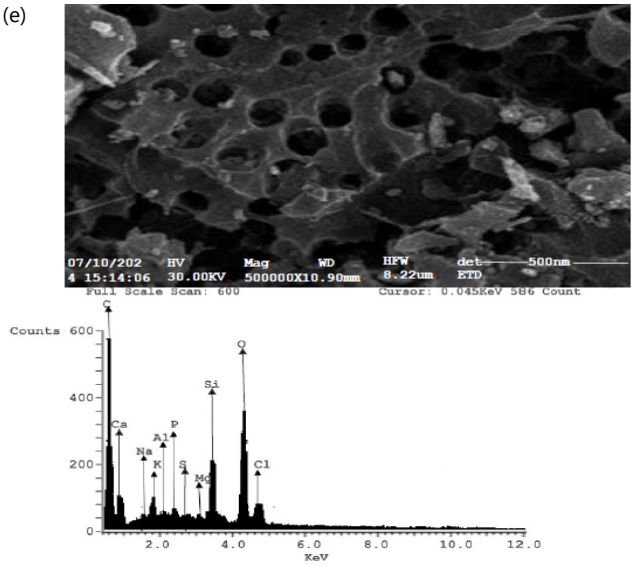


| Elements | Composition (%) |
|---|---|
| C | 67.07 |
| O | 18.81 |
| Ca | 1.04 |
| Si | 6.41 |
| Al | 0.23 |
| K | 2.71 |
| Na | 1.26 |
| Mg | 0.22 |
| P | 0.61 |
| Cl | 1.56 |
| S | 0.07 |

(f)

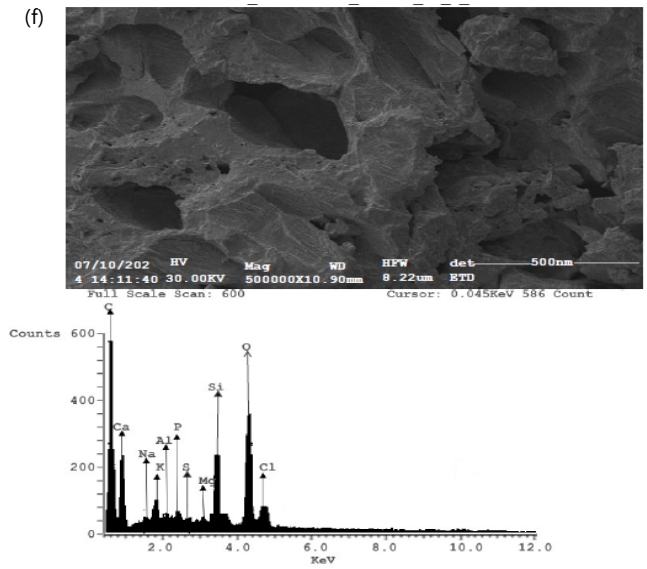


| Elements | Composition (%) |
|---|---|
| C | 64.66 |
| O | 15.92 |
| Ca | 1.70 |
| Si | 7.92 |
| Al | 1.50 |
| K | 2.54 |
| Na | 1.75 |
| Mg | 1.06 |
| P | 1.10 |
| Cl | 1.80 |
| S | 0.04 |

Fig 5(a-f): SEM/EDX of coconut shell biochar samples prepared at different heat treatment temperatures (a) BC350 (b) BC400 (c) BC450 (d) BC500 (e) BC600 and (f) BC700

The surface morphology reveals a porous, cellular structure (scale bar = 500 nm). Imaging was performed at an accelerating voltage of 30.00 kV and a magnification of 500,000x

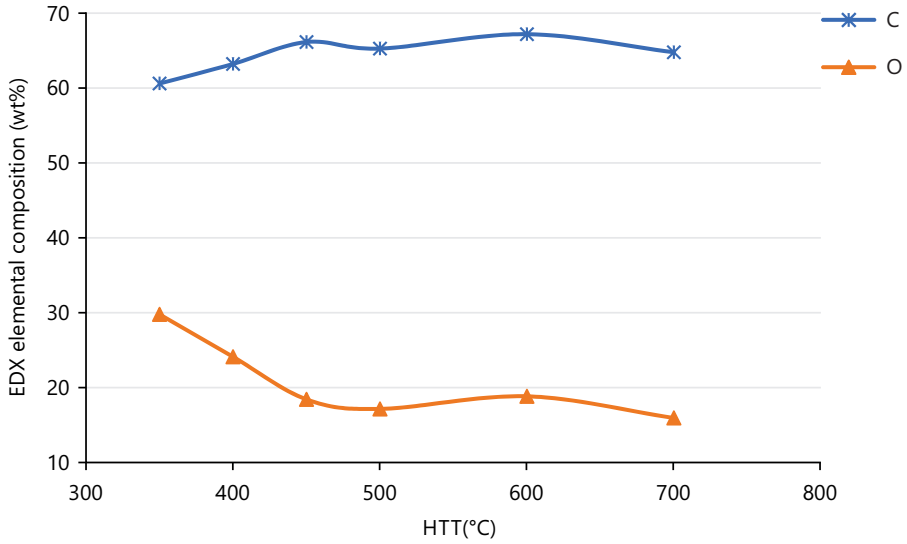


Fig. 6: Effect of heat treatment temperature (HTT) on C and O contents (wt %) of coconut shell biochar Elemental composition

Table 1: Ultimate elemental composition of coconut shell biochar produced at different heat treatment temperatures

| | Ultimate Composition (wt%) | | | | |
|---|---|---|---|---|---|
| Samples | C | H | O | N | S |
| CSB350 | 60.18±0.02 | 3.03±0.02 | 36.14±0.03 | 0.41±0.02 | 0.22±0.02 |
| CSB400 | 61.39±0.02 | 2.99±0.02 | 33.85±0.06 | 0.48±0.00 | 0.24±0.01 |
| CSB450 | 62.92±0.02 | 2.61±0.02 | 33.76±0.00 | 0.57±0.02 | 0.14±0.02 |
| CSB500 | 63.95±0.03 | 2.53±0.03 | 33.75±1.78 | 0.59±0.00 | 0.40±0.00 |
| CSB600 | 65.01±0.00 | 2.43±0.02 | 33.37±0.00 | 0.93±0.01 | 0.083±0.01 |
| CSB700 | 68.63±0.01 | 2.30±0.02 | 27.36±0.04 | 0.98±0.03 | 0.037±0.01 |

CSB: Coconut shell biochar, Ultimate composition expressed in weight percentage (wt%) with Mean±Standard Deviation (n = 3), C: Carbon, H: Hydrogen, O: Oxygen, N: Nitrogen and S: Sulfur

**Surface morphology:** Scanning electron, and electron dispersive X-ray micrographs of the biochar samples are shown in Fig. 5a-f. The scanning electron microscope (SEM) images show that the coconut biochar samples have random shape structures with a range of particle size distribution with deep pores that became more prominent with increase in pyrolysis temperature[31]. The pore structure can be seen to have collapsed at higher pyrolysis temperature (700°C) due to volatilization of organic material and increase carbonization. These porous structures and the change in the shape and size are associated with the improvement in the properties of biochar are useful in multifunctional application.

It can be seen that carbon and oxygen are the major elemental components of the biochar samples. The variation of the surface C and O contents of the biochar samples are shown in Fig. 6. The increase in C content of biochar with increase in heat treatment temperature is in contrast with the observed decrease in biochar yield with increase in heat treatment temperature Fig 2a. Therefore, pyrolysis of biomass at higher temperature range (≥600°C) may be required for biochar with high C content that may be required for carbon sequestration applications. Fig. 5 showed that the O content of the biochars decreased with increase in volatilization and loss of surface oxygen functional groups with increase in heat treatment temperature as observed in Fig. 3. The levels of other elements, particularly the mineral nutrient elements (Ca, Na, K, Mg and P) in the biochar samples are relatively low, and the total levels (sum of the mineral nutrient elements) increased with increase in heat treatment temperature from 8.52% at 350°C to 8.15% at 700°C due to the release of the mineral nutrients at higher heat treatment temperature to the biochar.

**Elemental composition:** The Carbon, Hydrogen, Nitrogen, Oxygen and Sulphur (CHNSO) contents of the biochar samples obtained at different heat treatment temperatures of coconut shell is given in Table 1.

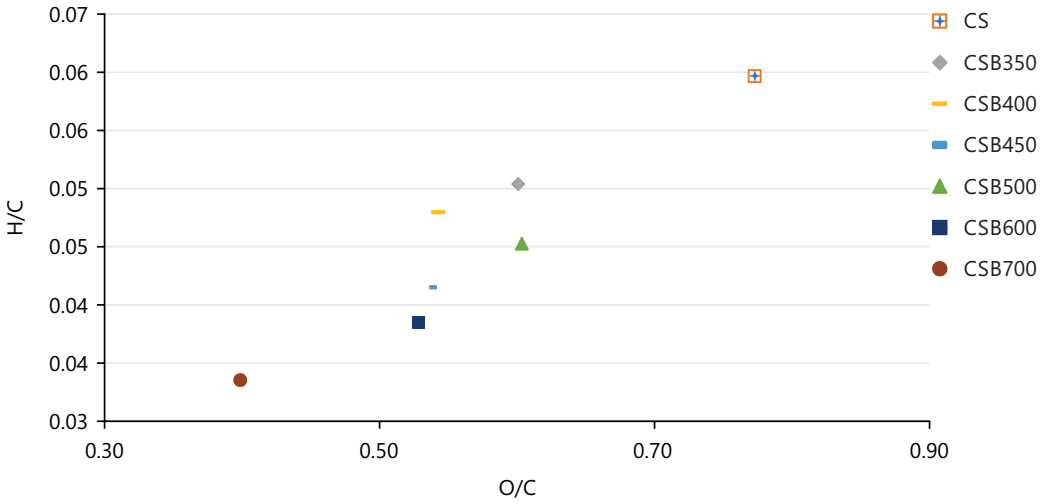


Fig. 7: van Krevelen plots of coconut shell biochar prepare at different heat treatment temperatures

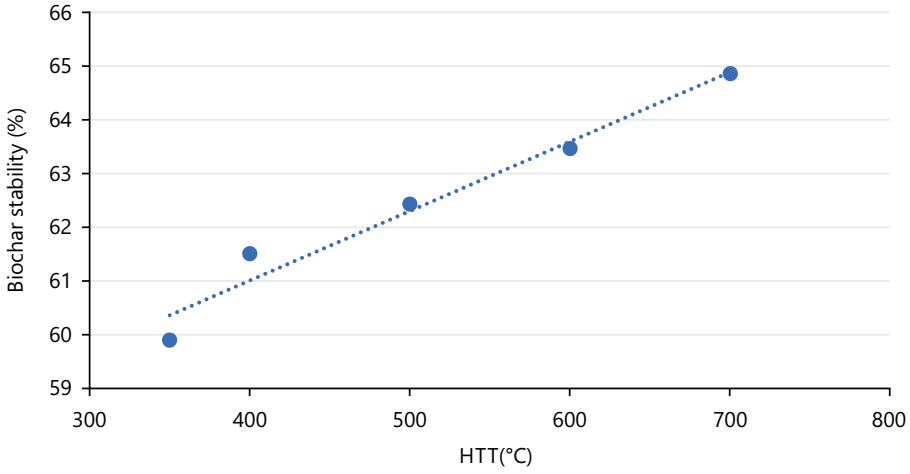


Fig 8: Chemical oxidation stability of coconut shell biochar produced at different heat treatment temperatures (HTT)

Table 1 shows that the C and N contents of biochar samples increased with increase in heat treatment temperature, while the H, S, and O contents decrease with increase in temperature. This trend is similar to trend in previous reports where explanations were offered in terms of increased dehydration and deoxygenation reactions culminating in the loss of H and O, and accumulation of C in the residual biochar associated with increase in heat treatment temperature[32]. The N and S contents of the biochar samples also decreased with increase in heat treatment temperature. The H:C and O:C molar ratios follow similar trend: Decreased with increase in heat treatment temperature. The (Table 1) and are shown in as van Krevelen plot (Fig. 7) which indicates clearly that the values of H:C and O:C are highest for the unpyrolysed coconut shell and lowest for the biochar samples obtained at 700°C.

The H:C ratio is often considered a good indicator of the average H-C bonds and size of polyaromatic graphene clusters. The values of H:C ratio for the biochar samples are within the range that designates stable structure with carbon sequestration potential[33]. The values of O:C decrease with an increase in heat treatment temperature with values for biochar at 600 and 700°C as low as 0.38 and 0.30, suggesting that the half-life of the samples are in the range of 100-1000 years[34], and with considerable carbon sequestration potential.

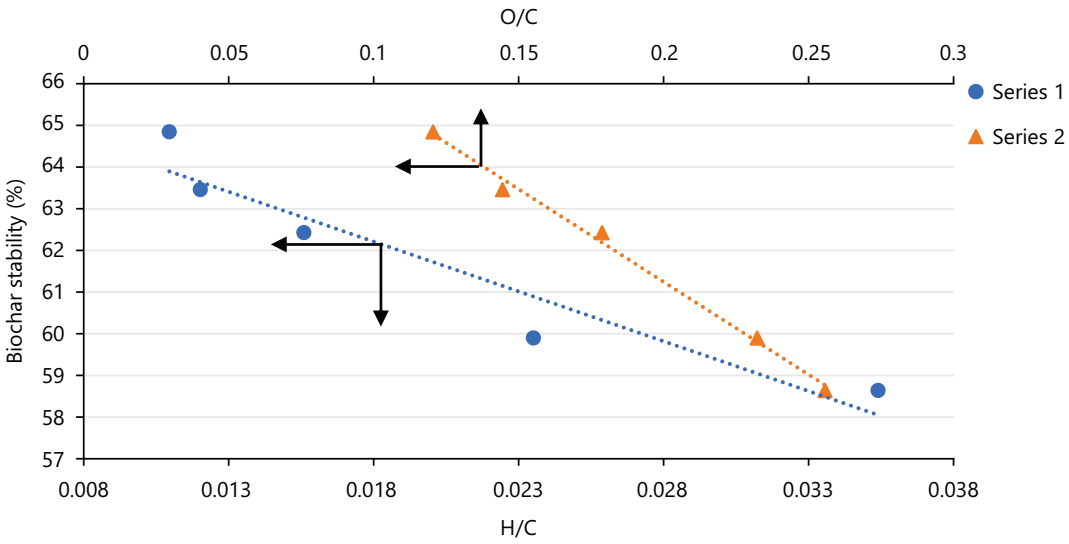


Fig. 9: Correlation of indicators of biochar stability
O:C: Atomic oxygen-to-carbon ratio and H:C: Atomic hydrogen-to-carbon ratio

**Chemical oxidation stability:** The carbons in pyrolytic biochars can either be unstable/labile or stable/recalcitrant depending on the biomass source and heat treatment temperature. The stable forms of carbon in biochar are responsible for its inherent value in carbon sequestration application. Chemical oxidation (accelerated aging) provides a direct method for the determination of the stability of biochar.

Figure 8 shows the effect of heat treatment temperature on chemical oxidative stability of coconut shell biochars. It can be seen that higher heat treatment temperatures produced biochars with greater stability, corroborating the results from the H:C and O:C ratios presented in Fig. 9. These results suggest that heat treatment temperatures (≥600°C) may be required to prepare biochars of requisite chemical oxidation stability for carbon sequestration applications.

## CONCLUSION

This study revealed that slow pyrolysis of coconut shell was associated with evolution of physicochemical and textural properties, surface morphology, elemental composition, and chemical oxidative stability of coconut shell was reported in this study. It can be concluded that pyrolysis at mid-range temperatures (400-500°C) at which important physicochemical properties: Cation exchange capacity, electrical conductivity, total surface oxygen functional groups, and textural properties: Specific surface area and pore volume were accentuated, may be used to prepare coconut shell biochar, requisite agronomic benefits. On the other hand, higher heat treatment temperatures (≥600°C) allowed for the evolution of biochar structures that are stable, recalcitrant and suitable for carbon sequestration applications.

## SIGNIFICANCE STATEMENT

This study demonstrates that optimizing pyrolysis temperature significantly enhances the stability and carbon sequestration potential of coconut shell biochar, making it an effective long-term soil amendment. The findings provide valuable insights for sustainable waste management and climate change mitigation by converting agricultural residues into stable carbon-rich materials. Additionally, the identified relationships between temperature, surface properties, and carbon stability offer practical guidance for large-scale biochar production and its application in improving soil health and reducing atmospheric carbon levels.

## ACKNOWLEDGMENT

The authors are sincerely grateful to the Department of Chemistry, University of Benin, Benin, Nigeria for allowing us use some of their facilities.

**REFERENCES**


1. Kan, T., V. Strezov and T.J. Evans, 2016. Lignocellulosic biomass pyrolysis: A review of product properties and effects of pyrolysis parameters. Renew. Sustainable Energy Rev., 57: 1126-1140.
2. Dhyani, V. and T. Bhaskar, 2019. Pyrolysis of Biomass. In: Biofuels: Alternative Feedstocks and Conversion Processes for the Production of Liquid and Gaseous Biofuels, Pandey, A., C. Larroche, C.G. Dussap, E. Gnansounou, S.K. Khanal and S. Ricke (Eds.), Elsevier, Amsterdam, Netherlands, ISBN: 978-0-12-816856-1, pp: 217-244.
3. Zhou, X., Y. Zhu, Q. Niu, G. Zeng and C. Lai *et al*., 2021. New notion of biochar: A review on the mechanism of biochar applications in advannced oxidation processes. Chem. Eng. J., Vol. 416. 10.1016/j.cej.2021.129027.
4. de Almeida, S.G.C., L.A.C. Tarelho, T. Hauschild, M.A.M. Costa and K.J. Dussán, 2022. Biochar production from sugarcane biomass using slow pyrolysis: Characterization of the solid fraction. Chem. Eng. Process. Process Intensif., Vol. 179. 10.1016/j.cep.2022.109054.
5. Fan, J., T. Duan, L. Zou and J. Sun, 2023. Characteristics of dissolved organic matter composition in biochar: Effects of feedstocks and pyrolysis temperatures. Environ. Sci. Pollut. Res., 30: 85139-85153.
6. Keiluweit, M., P.S. Nico, M.G. Johnson and M. Kleber, 2010. Dynamic molecular structure of plant biomass-derived black carbon (biochar). Environ. Sci. Technol., 44: 1247-1253.
7. Gupta, S., G.K. Gupta and M.K. Mondal, 2019. Slow pyrolysis of chemically treated walnut shell for valuable products: Effect of process parameters and in-depth product analysis. Energy, 181: 665-676.
8. Chang, J., H. Zhang, H. Cheng, Y. Yan and M. Chang *et al*., 2020. Spent *Ganoderma lucidum* substrate derived biochar as a new bio-adsorbent for $Pb^{2+}$/$Cd^{2+}$ removal in water. Chemosphere, Vol. 241. 10.1016/j.chemosphere.2019.125121.
9. Wang, J., Z. Li, Y. Li, Z. Wang, X. Liu, Z. Liu and J. Ma, 2024. Evolution and correlation of the physiochemical properties of bamboo char under successive pyrolysis process. Biochar, Vol. 6. 10.1007/s42773-024-00321-6.
10. Ma, Z., Y. Yang, Q. Ma, H. Zhou, X. Luo, X. Liu and S. Wang, 2017. Evolution of the chemical composition, functional group, pore structure and crystallographic structure of bio-char from palm kernel shell pyrolysis under different temperatures. J. Anal. Appl. Pyrolysis, 127: 350-359.
11. Pradhan, S., A.H. Abdelaal, K. Mroue, T. Al-Ansari, H.R. Mackey and G. McKay, 2020. Biochar from vegetable wastes: Agro-environmental characterization. Biochar, 2: 439-453.
12. Lehmann, J. and S. Joseph, 2015. Biochar for Environmental Management: An introduction. In: Biochar for Environmental Management: Science, Technology and Implementation, Lehmann, J. and S. Joseph (Eds.), Routledge, Abingdon, Oxfordshire, ISBN: 9780203762264, pp: 1-13.
13. Ajien, A., J. Idris, N.M. Sofwan, R. Husen and H. Seli, 2022. Coconut shell and husk biochar: A review of production and activation technology, economic, financial aspect and application. Waste Manage. Res., 41: 37-51.
14. Jain, N., A. Bhatia and H. Pathak, 2014. Emission of air pollutants from crop residue burning in India. Aerosol Air Qual. Res., 14: 422-430.
15. Naeem, M.A., M Khalid, M. Arshad and R. Ahmad, 2014. Yield and nutrient composition of biochar produced from different feedstocks at varying pyrolytic temperatures. Pak. J. Agric. Sci., 51: 75-82.
16. Mukherjee, A., A.R. Zimmerman and W. Harris, 2011. Surface chemistry variations among a series of laboratory-produced biochars. Geoderma, 163: 247-255.
17. Ahmedna, M., M.M. John, S.J. Clarke, W.E. Marshal and R.M. Rao, 1997. Potential of agricultural by-product-based activated carbons for use in raw sugar decolourisation. J. Sci. Food Agric., 75: 117-124.
18. Othugile, L.E., T. Lekgoba and F. Ntuli, 2022. Sequestration of heavy metals from coal wash water using biochar from pyrolysis of morula shells. Eur. J. Sustainable Dev. Res., Vol. 6. 10.21601/ejosdr/11377.
19. Aimikhe, V.J., M.S. Anyebe and M. Ibezim-Ezeani, 2024. Development of composite activated carbon from mango and almond seed shells for $CO_2$ capture. Biomass Convers. Biorefin., 14: 4645-4659.
20. Shoaib, A.G.M., A. El-Sikaily, A. El Nemr, A.E-D.A. Mohamed and A.A. Hassan, 2022. Preparation and characterization of highly surface area activated carbons followed type IV from marine red alga (*Pterocladia capillacea*) by zinc chloride activation. Biomass Convers. Biorefin., 12: 2253-2265.

21. Gazulla, M.F., M. Rodrigo, M. Orduña and M.J. Ventura, 2016. Determination of organic oxygen in petroleum cokes and coals. Microchem. J., 126: 538-544.
22. Tirol-Padre, A. and J.K. Ladha, 2004. Assessing the reliability of permanganate-oxidizable carbon as an index of soil labile carbon. Soil Sci. Soc. Am. J., 68: 969-978.
23. Fidel, R.B., D.A. Laird, M.L. Thompson and M. Lawrinenko, 2017. Characterization and quantification of biochar alkalinity. Chemosphere, 167: 367-373.
24. Cross, A. and S.P. Sohi, 2013. A method for screening the relative long-term stability of biochar. GCB Bioenergy, 5: 215-220.
25. Noor, N.M., A. Shariff, N. Abdullah and N.S.M. Aziz, 2019. Temperature effect on biochar properties from slow pyrolysis of coconut flesh waste. Malays. J. Fundam. Appl. Sci., 15: 153-158.
26. Cantrell, K.B., P.G. Hunt, M. Uchimiya, J.M. Novak and K.S. Ro, 2012. Impact of pyrolysis temperature and manure source on physicochemical characteristics of biochar. Bioresour. Technol., 107: 419-428.
27. Tu, P., G. Zhang, G. Wei, J. Li, Y. Li, L. Deng and H. Yuan, 2022. Influence of pyrolysis temperature on the physicochemical properties of biochars obtained from herbaceous and woody plants. Bioresour. Bioprocess., Vol. 9. 10.1186/s40643-022-00618-z.
28. Ortiz, L.R., E. Torres, D. Zalazar, H. Zhang, R. Rodriguez and G. Mazza, 2020. Influence of pyrolysis temperature and bio-waste composition on biochar characteristics. Renewable Energy, 155: 837-847.
29. Weber, K. and P. Quicker, 2018. Properties of biochar. Fuel, 217: 240-261.
30. Ogede, L.O., C.M. Ejimadu and F.E. Okieimen, 2024. Chemical and textural properties of melon seed shell-derived biochar relevant to their application in the remediation of contaminated soil. Niger. Res. J. Eng. Environ. Sci., 9: 681-688.
31. Elnour, A.Y., A.A. Alghyamah, H.M. Shaikh, A.M. Poulose, S.M. Al-Zahrani, A. Anis and M.I. Al-Wabel, 2019. Effect of pyrolysis temperature on biochar microstructural evolution, physicochemical characteristics, and its influence on biochar/polypropylene composites. Appl. Sci., Vol. 9. 10.3390/app9061149.
32. Chen, Y., H. Yang, X. Wang, S. Zhang and H. Chen, 2012. Biomass-based pyrolytic polygeneration system on cotton stalk pyrolysis: Influence of temperature. Bioresour. Technol., 107: 411-418.
33. Crombie, K., O. Mašek, S.P. Sohi, P. Brownsort and A. Cross, 2013. The effect of pyrolysis conditions on biochar stability as determined by three methods. GCB Bioenergy, 5: 122-131.
34. Jeffery, S., F.G.A. Verheijen, M. van der Velde and A.C. Bastos, 2011. A quantitative review of the effects of biochar application to soils on crop productivity using meta-analysis. Agric. Ecosyst. Environ., 144: 175-187.